

## The synthesis of TiO<sub>2</sub> thin film by Chemical Bath Deposition (CBD) method

A. Elfanaoui<sup>1\*</sup>, A. Ihlal<sup>1</sup>, A. Taleb<sup>2</sup>, L. Boulkaddat<sup>1</sup>, E. Elhamri<sup>1</sup>, M. Meddah<sup>1</sup>, K. Bouabid<sup>1</sup> and X. Portier<sup>3</sup>

<sup>1</sup>Laboratory of Materials and Renewable Energies (LMRE), University Ibn Zohr Physical Dep., Faculty of sciences P B.8106, Hay Dakhla, 80000 Agadir, Morocco.

<sup>2</sup>UPMC-LECIME/ENSCP ParisTech/CNRS-UMR7575 11, rue Pierre et Marie Curie, 75231 Paris cedex 05.

<sup>3</sup>CIMAP, Ensicaen, Bd du Maréchal Juin, 14050 Caen, France.

\*Corresponding authors: elfanaouiha@yahoo.fr

**Abstract :** Titanium oxide (TiO<sub>2</sub>) films have several advantages for applications in solar cells and very commonly used as a photocatalyst for degradation of environmental pollutants. In this study, TiO<sub>2</sub> films were synthesized using, a simple, less expensive, low temperature and convenient for large area deposition method, a chemical bath deposition (CBD) and their structural and optical properties were examined at various calcination temperatures.

The X-ray diffraction (XRD) technique shows the presence of the peaks characteristic of anatase phase after annealing our films at 500°C, 600°C and rutile phase appears after heat treatment at 700°C. The surface morphology of the deposited films was characterized by the FEG scanning electron microscopy (FEGSEM) and atomic force microscopy (AFM). Energy dispersive X-ray spectroscopy (EDS) analysis was used to determine the chemical composition of the prepared films. The UV-Vis-NIR spectroscopy shows that the film exhibits a transmission around 60%. The indirect band gap of the deposited films was between 2.88 and 3.22 eV.

**Keywords :** titanium dioxide, chemical bath deposition; optical band gap and anatase

### Introduction

Titanium dioxide (TiO<sub>2</sub>) is a widely used material for optical and protective applications because of its high transparency in the visible region, excellent mechanical durability [1] and chemical stability in aqueous solution [2]. TiO<sub>2</sub> films are useful for such applications as catalysis [3], optical coatings, gas sensors [4], and other electronic devices [5]. TiO<sub>2</sub> films have been prepared by a variety of chemical and physical deposition techniques, such as the sol-gel process [6, 8], chemical vapor deposition [9], and chemical bath deposition [10, 11] atomic layer deposition [12], evaporation [13], various reactive sputtering methods [14, 15], ion beam assisted processes [16], pulse laser deposition [17].

It is known that the physical properties of the TiO<sub>2</sub> material strongly depend on the deposition method and calcination temperatures. In general TiO<sub>2</sub> films transform from amorphous to anatase and then to rutile depending on the calcination temperature. There are reports about the dependence of annealing temperature on structural and optical properties (Lottiaux et al., 1989; Kin et al., 2002; Houet al., 2003).

In our previous work, we have studied the effect of the annealing temperature on the structural and optical properties of the TiO<sub>2</sub> thin films prepared by sol-gel method [7, 18, 19]. In the present work, we present our contribution in the study of properties of TiO<sub>2</sub> thin films prepared by the low cost and easily adaptable to industry scale technique "chemical bath deposition" on glass substrate.

### Experimental procedure

In order to synthesize the TiO<sub>2</sub> thin films, the peroxo-titanium precursor was prepared in the aqueous acidic medium by mixing TiOSO<sub>4</sub> powder and H<sub>2</sub>O<sub>2</sub> with constant stirring for 25 min to get a red clear solution [20]. The obtained solution was kept in the bath at room temperature with constant stirring. The glass substrate was cleaned in an ultrasonic bath with acetone and ethanol solution, and then rinsed with bidistilled water and finally purged with nitrogen gas. The glass substrates were immersed vertically in the solution. After 12 h deposition time, the substrates were withdrawn from the solution, sufficiently rinsed with the double-distilled water and purged with nitrogen gas at room temperature (25 °C). The films were then dried at 100 °C for 1 h and subsequently annealed at 500°C, 600 °C and 700°C in air during 1 h. The by-product powder was collected through filtering, washed, dried, and submitted for further characterization.

The morphological investigations of the prepared films were achieved with a high-resolution Ultra 55 Zeiss FEG scanning electron microscope (FEGSEM) operating at an acceleration voltage of 10 kV. Atomic force microscopy (AFM) measurements were performed at room temperature using a Nanoscope III instrument in a standard tapping mode to investigate the surface morphology of TiO<sub>2</sub> films. Energy dispersive X-ray spectroscopy (EDX) analyses were used to determine the chemical composition of the prepared films and realized in FEGSEM using a PGT spirit energy dispersive spectrometry system (EDS).

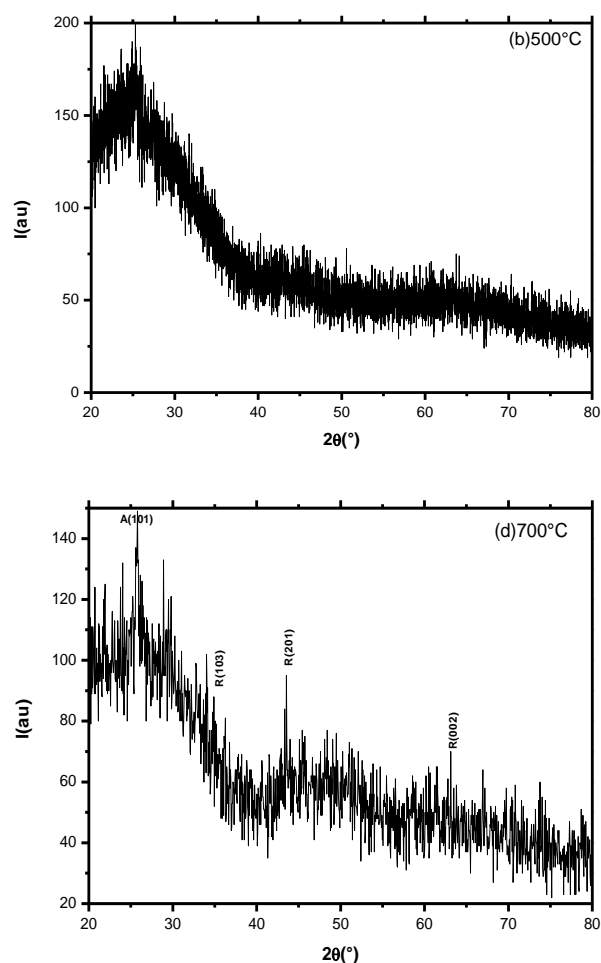
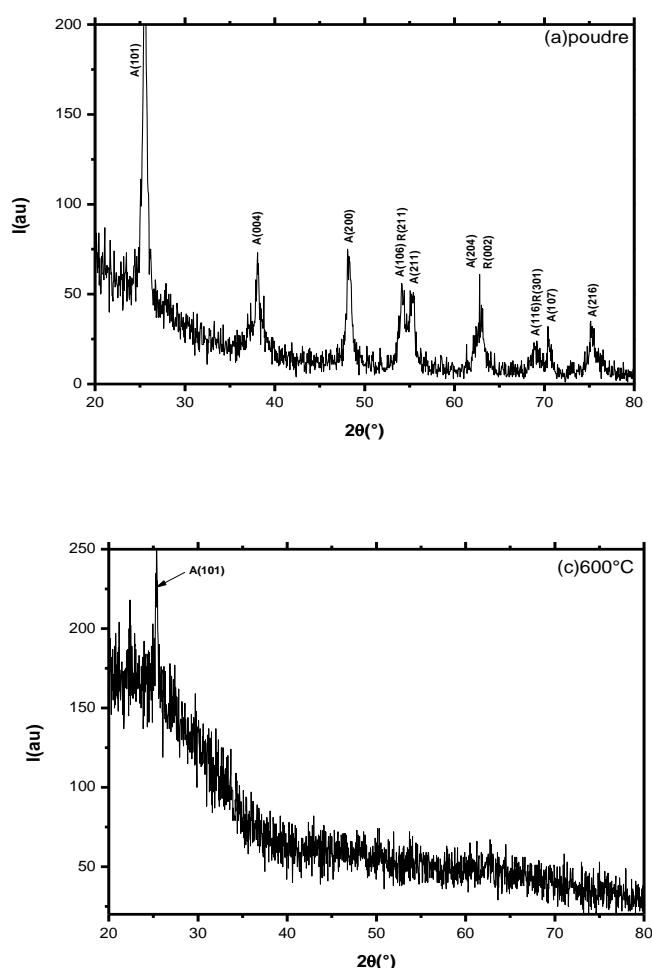
The crystalline structure was determined by an X-ray diffractometer (XPERT-PRO) in  $2\theta$  range from  $20^\circ$  to  $80^\circ$  by  $0.03^\circ \text{ s}^{-1}$  increasing steps operating at 35 KV accelerating voltage and 30 mA current using  $\text{CuK}\alpha$  radiation source with  $\lambda = 1.5406 \text{ \AA}$ .

The optical measurements were performed using a Shimadzu UV-Vis-NIR-3101 PC spectrophotometer operating at normal incidence in the wavelength range from 300 nm to 800 nm. A glass substrate cleaned with the same procedure described above was used as reference.

## Results and discussions

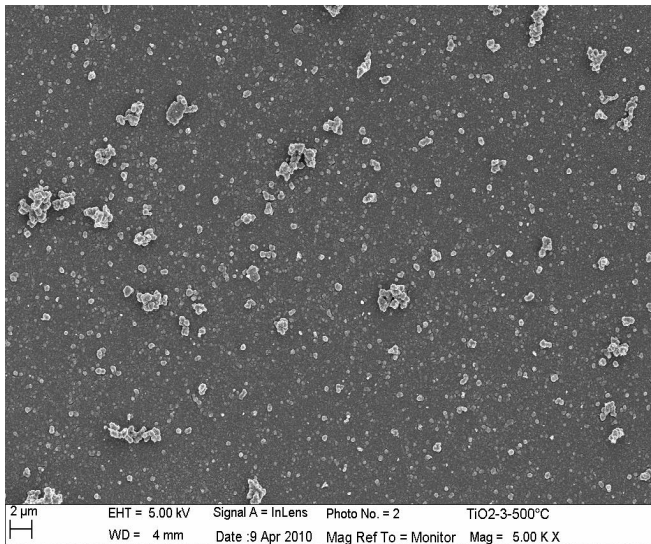
### I. Crystallographical and morphological analyses

$\text{TiO}_2$  has three well-known phases namely: anatase, rutile, and brookite [21]. Rutile and anatase are tetragonal whereas brookite is orthorhombic. Rutile is the only stable phase. Anatase and brookite are metastable at all temperatures, and can be converted to rutile after heat treatment at high temperature.



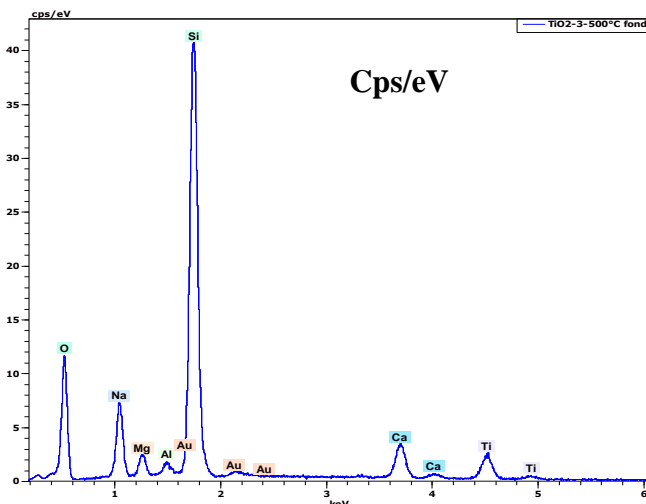
**Figure 1: The XRD pattern of  $\text{TiO}_2$  powder (a) and  $\text{TiO}_2$  films deposited on the glass substrate annealed at (b)  $500^\circ\text{C}$ , (c)  $600^\circ\text{C}$  and (d)  $700^\circ\text{C}$**

Figure 1 shows XRD pattern of (a) the collected by-product of  $\text{TiO}_2$  annealed at  $500^\circ\text{C}$  for 1 h in air, and  $\text{TiO}_2$  thin films deposited on the glass substrate using the CBD method and heat-treated for 1 hour at (b)  $500^\circ\text{C}$ , (c)  $600^\circ\text{C}$  and (d)  $700^\circ\text{C}$ . It is clear that in the case of  $\text{TiO}_2$  powder both anatase and rutile structures are present with special spots, whereas in the case of  $\text{TiO}_2$  thin film annealed at  $500^\circ\text{C}$  and  $600^\circ\text{C}$  there is less peaks characteristic of anatase phases this observation is in good agreement with the previous works of other researchers [21, 24]. When the annealing temperature reached  $700^\circ\text{C}$  the rutile phase appears. Anatase-rutile transformation occurred after annealing at  $700^\circ\text{C}$ , this conclusion was mentioned in the literature by Nakaruk et al. [25], Sankar et al. [26], Wiggins et al. [27] and Okimura et al [28]. The crystallite size, for  $\text{TiO}_2$  thin film annealed at  $500^\circ\text{C}$ ,  $600^\circ\text{C}$  and  $700^\circ\text{C}$ , has been estimated from the full-width at half-maximum (FWHM) of the (101) diffraction peak by using Scherrer's equation [29] about respectively 47 nm, 25 nm and 11 nm.



**Figure 2: Micrograph FEGSEM of the TiO<sub>2</sub> thin film deposited on the glass substrate annealed at 500°C**

In Figure 2, we present the FEGSEM image of the TiO<sub>2</sub> thin film annealed at 500°C. The films cover the whole substrate and show a rough surface, no pinholes and granular texture with clearly identified grain at the surface. The energy dispersive X-ray spectroscopy (EDS) analysis in Fig. 3 reveals the existence of Ti and O elements on the surface of annealed films and other chemical species coming from the glass substrate. Unfortunately no quantitative analyses were performed on our samples.



**Figure 3: The energy dispersive X-ray (EDS) analysis of TiO<sub>2</sub> thin film annealed at temperature of 500°C**

Figure 4 shows the AFM images 2D and 3D of TiO<sub>2</sub> thin film annealed at 500°C. These micrographs show that the thin films of TiO<sub>2</sub> has homogeneous surfaces morphology with spherical particles of regular size and uniform distribution. The mean roughness measured for this sample was 3.95 nm.

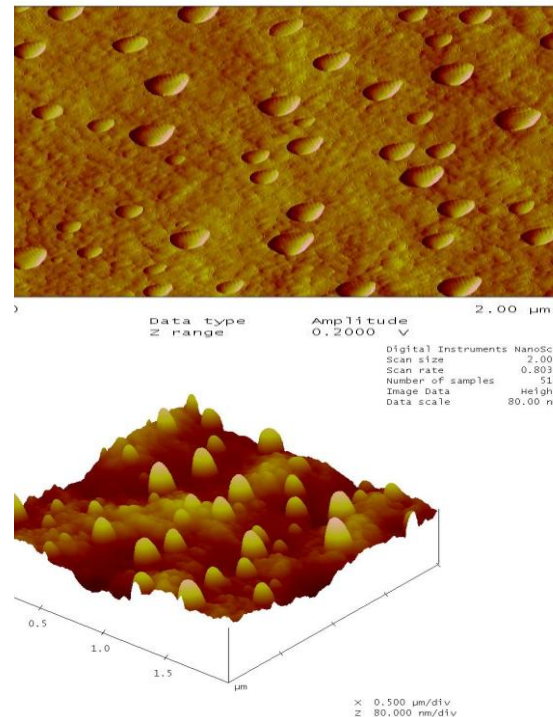


**Figure 4 : 3D and 2D AFM images of TiO<sub>2</sub> thin film recorded on the aggregates shown in Fig. 3**

## II. Optical analysis of TiO<sub>2</sub> films

Figure 5 shows the transmittance spectra of a typical TiO<sub>2</sub> thin film annealed at 500°C, 600°C and 700°C over the spectral range of 300–800 nm. The average optical transmittance of the film is near 50% in the visible range for the thin film annealed at 500°C and increase to 75 % when the annealing temperature reached 600°C and then decreased to 50% when the thin film is annealed at 700°C. The increase in transmittance with temperature is related to the increase of grain size and a reduction of the grain boundary scattering. This is the Burstein–Moss shift related to the electron density [30, 31]

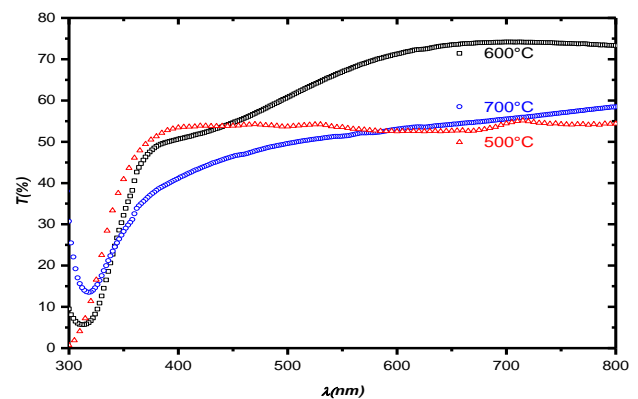


**Figure 5: Optical transmission spectra of TiO<sub>2</sub> thin films deposited on the glass substrate and annealed at 500°C, 600°C and 700°C**

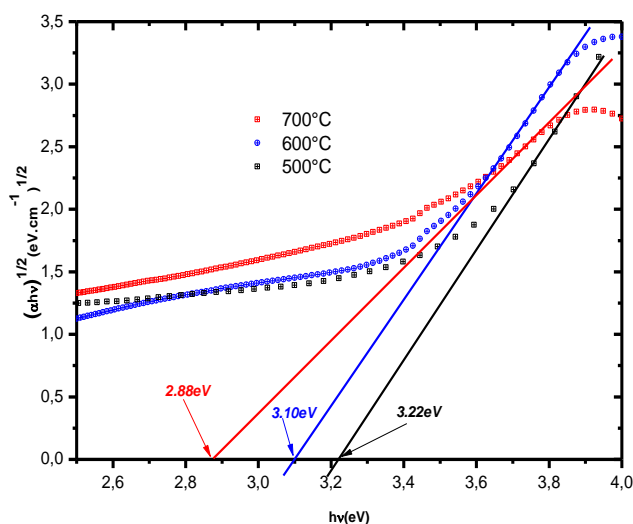


**Figure 6:** The  $(\alpha hv)^{1/2}$  versus  $h\nu$  plots of  $\text{TiO}_2$  thin films annealed at 500°C, 600°C and 700°C

The optical band gap of  $\text{TiO}_2$  film can be determined from the sharply falling transmission region. According to Tauc equation below [32], the absorption coefficient has the following energy dependence (Eq. (2)):

$$\alpha hv = B(h\nu - E_g)^n \quad (1)$$

Where  $h\nu$  is the incident photon energy, B the edge width parameter and n an exponent that determines the type of electronic transition causing absorption, which is 1/2 or 2 for direct or indirect transition, respectively. Transmittance data was found to fit for  $n = 2$  as shown in Figure 6, meaning that the type of electronic transitions causing absorption is indirect allowed. Band gap energy,  $E_g$ , of the films can be obtained by extrapolating the linear region of the plot  $(\alpha hv)^{1/2}$  to zero absorption coefficient i.e.  $\alpha = 0$ . The estimated indirect band gap energy ( $E_{g,\text{ind}}$ ) of  $\text{TiO}_2$  decreases from 3.22 eV to 2.88 eV by increasing of the annealing temperature from 500°C to 700°C. The increase of  $E_g$  is attributed to a reduction of the oxygen vacancies with increasing of annealing temperature [33]. These values are in good agreement with the literature values for the  $\text{TiO}_2$  thin films [34, 35].

## Conclusion

$\text{TiO}_2$  thin films were grown on glass substrates by the chemical bath deposition using  $\text{TiOSO}_4$  as a precursor, and annealed at high temperature 500°C, 600°C and 700°C. The structural and optical properties of the thin films of  $\text{TiO}_2$  were explored using different characterization techniques. Structural analysis revealed the presence of the anatase and rutile structures depending on the heat treatment and the surface is uniform with small grains. Optical study shows that the optical transmission reached 60% in the visible range and the indirect optical band-gap was estimated to be between 2.88 eV to 3.22 eV. Such

features allow the  $\text{TiO}_2$  films to be an interesting partner as a buffer or window layer in thin film based solar cells.

## Acknowledgment

This work was partially supported by the CNRST/CNRS cooperation program (Chimie 05/08, SPM05/09 and SPM05/10).

## Reference

- [1]. M. Okada, Y. Yamada, P. Jin, M. Tazawa, K. Yoshimura, *Thin Solid Films*, 442 (2003) 217.
- [2]. A. Ennaoui, B. R. Sankapal, V. Skryshevsky, M. C. L. Steiner, *Sol. Energy Mater. Sol. Cells*, 90 (2006) 1533.
- [3]. R. Weinberger, R. B. Garber, *Appl. Phys. Lett.*, 66 (1995) 2409.
- [4]. D. Manno, G. Micocci, R. Rella, A. Serra, A. Taurino, A. Tepore, *J. Appl. Phys.*, 82 (1997) 54.
- [5]. Z. Wang, X. Hu, *Thin Solid Films*, 352 (1999) 62.
- [6]. J. X. Liu, D. Z. Yang, F. Shi, Y. J. Cai, *Thin Solid Films*, 429 (2003) 225.
- [7]. A. Elfanaoui, E. Elhamri, L. Boulkaddat, A. Ihlal, K. Bouabid, L. Laanab, A. Taleb, X. Portier, *International journal of hydrogen energy*, 36 (2011) 4130-4133.
- [8]. A. Bendavid, P. J. Martin, H. Takikawa, *Thin Solid Films*, 360 (2000) 241.
- [9]. L. M. Williams, D. W. Hess, *J. Vac. Sci. Technol. A* 1 (1983) 1810.
- [10]. S. Suzuk, I. Ohsak, N. Ando, *Jpn. J. Appl. Phys.*, 35 (1996) 1862.
- [11]. A. Elfanaoui, L. Boulkaddat, A. Taleb, A. Ihlal, E. Elhamri, M. Meddah, K. Bouabid, X. Portier, *Ann. Chim. Sci. Mat.*, 36(1) (2011) 37.
- [12]. J. Aarik, A. Aiala, A. A. Kiisler, T. Uustare, V. Sammelselg, *Thin Solid Films*, 305 (1997) 270.
- [13]. T. Fujii, N. Sakata, J. Takada, Y. Miura, Y. Daitoh, M. Takano, *J. Mater. Res.*, 9 (1994) 1468.
- [14]. S. B. Amor, G. Baud, J. P. Besse, M. Jacquet, *Thin Solid Films*, 293 (1997) 163.
- [15]. K. Okimura, A. Shibata, N. Maeda, K. Tachibana, Y. Noguchi, K. Tsuchida, *Jpn. J. Appl. Phys.*, 34 (1995) 4950.
- [16]. M. Gilo, N. Croitoru, *Thin Solid Films*, 283 (1996) 84.
- [17]. M. Mosaddeq-ur-Rahman, G. Yu, K. M. Krishna, T. Soga, J. Watanabe, T. Jimbo, M. Umeno, *Appl. Opt.*, 37 (1998) 691.
- [18]. K. Bouabid, A. Ihlal, Y. Amira, A. Sdaq, A. Assabane, Y. Ait-Ichou, A. Outzourhit, E. L. Ameziane, and G. Nouet, *Ferroelectrics*, 372 (2008), 69-75.
- [19]. L. Boulkaddat, A. Elfanaoui, E. Elhamri, M. Meddah, A. Ihlal, K. Bouabid, A. Benhachemi, L. Bazzi, X. Portier, *Global Journal of Physical Chemistry*, 2 (2011) 88.
- [20]. B. R. Sankapal, M. C. Lux-Steiner, A. Ennaoui, *Appl. Sur. Sci.*, 239 (2005) 165.
- [21]. I. Zhitomirsky, *J. Mater. Sci.* 34 (1999) 2441.
- [22]. S. Karuppuchamy, K. Nonomura, T. Yoshida, T. Sugiura, H. Minoura, *Solid State Ionics* 151 (2002) 19.
- [23]. R. S. Mane, S. J. Roh, O. S. Joo, C. D. Lokhande, S. H. Han, *Electrochem. Acta* 50 (2005) 2453.
- [24]. C. D. Lokhande, S. K. Min, K. D. Jung, O. S. Joo, *J. Mater. Sci.* 39 (2004) 6610.

- [25]. S. Sankar, K. G. Gopchandran, Indian Journal of Pure & Applied Physics, 46 (2008) 791-796.
- [26]. A. Nakaruk, D. Ragazzon, C.C. Sorrell, Thin Solid Films 518 (2010) 3735–3742.
- [27]. M.D. Wiggins, M.C. Neison, C. R. Aita, J. Vac. Sci. Technol. A14 3 (1996) 772-776.
- [28]. K. Okimura, A. Shibata, N. Maeda, K. Tachibana, Jpn. J. Appl. Phys. 34 (1995) 4950-4955.
- [29]. L. Meng, M. Dos Santos, Thin Solid Films 226 (1993) 22-29.
- [30]. S. Ray, R. Banerjee, N. Basu, A.K. Batabyal, A.K. Barua, J. Appl. Phys. 54 (1983) 3497.
- [31]. E. Burstein, Phys. Rev. 93 (1954) 632
- [32]. J.C. Tauc, Optical Properties of Solids, North-Holland, Amsterdam (1972), p. 372.
- [33]. F. F. Ngaffo, A. P. Caricato, F. Romano, Applied Surface Science 255 (2009) 9684–9687.
- [34]. Z. Yang, W. Liangzhuan, Z. Qinghui, Z. Jinfang, Materials Chemistry and Physics, 121 (2010) 235–240.
- [35]. W. Jianjun, L. Xujie, Z. Linlin, X. Yujuan, H. Fuqiang, X. Fangfang, Journal of Alloys and Compounds, 496 (2010) 234–240.